-

Simulation of Active Magnetic Bearing Response based NNC

Naseer Qassim Hamoody* & Adil Hameed Ahmad *

Received on : 21/4/2008
Accepted on : 9/10/2008

Abstract

The present work is dealing with the modeling, investigations, and controlling, of a prototype radial magnetic bearing system. Considerations based on the 8 poles model with switched mode power supply. Investigations of radial forces in two axes model and performance response are carried out through the intelligent controller system. Improving system response is achieved by using an efficient controller based Neural Network (NN) NARMA-L2 Controller together with the conventional PID controller. The response is presented for stand still and dynamic conditions using the implemented Simulink software. The results show that the NARMA-L2 is highly improved the dynamic response of the speeding up rotor in comparison with the conventional controller.

تمثيل استجابة الرافعات المغناطيسية باستخدام الشبكات العصبية الصناعية

الخلاصة

يتناول هذا البحث نمذجة ومحاكات والسيطرة على نموذج مقترح لرافع مغناطيسي للأحمال الأفقية الدوارة. النموذج المعتمد عبارة عن ثماني الأقطاب ذات مجهز قدرة متطور. تم استخدام مسيطر ذكي لدراسة ومحاكات القوى المغناطيسية الناتجة بالمحورين وكذلك اداء النموذج في حالة الأستقرار والحركة.لقد اثبتت النتائج ان استخدام المسيطر الذكي او المسيطر بالشبكة العصبية قد أعطى تحسين جيد في الاستجابة الحركية و أداء المنظومة عن حالة استخدام المسيطر الاعتيادي

https://doi.org/10.30684/etj.27.6.3

2412-0758/University of Technology-Iraq, Baghdad, Iraq

1. Introdution

Magnetic bearing (MB) is one of more important magnetic devices which has many applications with various fields to support the rotors without any mechanical contacts . It has been investigated by various researchers in the recent years [1]. There are two main types of magnetic bearings : Active Magnetic Bearing, and Passive Magnetic which supply currents to the electromagnets, a controller unit , and a gap sensors unit. The power amplifiers supply bias currents to the electromagnets, the constant levitating is mediated by the controller which offset the bias current as the rotor deviates by small amount from its center position. The gap sensors send shaft position signals to control system, which modulates the current in each electromagnet to vary its force and keep the rotor in its required position.

The power amplifiers in modern applications of MB are solid state devices. The controller is usually Proportional-Integral-Derivative (PID) controller, or in a digital techniques based on artificial intelligent to achieve the accurate in the MB operation.

Magnetic bearing provides increased availability, built in monitoring dynamic control of the rotor system, and allow direct-drive and variable speed capabilities. Very high control of shaft position gives the possibility of displacing the rotor inside the air gap.

Active MB can be divided into two main types according to their usage which are: Radial magnetic bearing; comprises a pair of electromagnetic poles to produce an attractive forces on the rotor in all directions, and Axial magnetic bearing; consists of axially symmetric electromagnets in the stator and a disc in the rotor.

Due to higher reliability and lower maintenance requirements, these systems are used in many drives environment and applications, such as gas production magnetic bearing for turbo-expander and direct coupled electric compressor, turbines, pumps, motor and generators. Magnetic Bearings are also used to support magnetic levitation of trains in order to get low noise and smooth ride by eliminating physical contact surfaces [3].

The evaluations of active magnetic bearing may be traced through the patents and research used in this field [4,5,6] . The history of Active Magnetic Bearing shows that the first commercial application of AMBs used in turbo machinery. In the present work, a Radial Active Magnetic Bearing (RAMB) is considered through the investigation and controlling performance for a prototype model.

2. Modeling and Formulation of Magnetic Bearing

The proposed radial magnetic bearing model is composed of four discrete horse shoe shaped electromagnets. The four magnets are arranged around a circular piece of iron (journal) mounted on the shaft (rotor) that is to be levitated. Each of the electromagnets can only produce a force that attracts the rotor iron , so all four electromagnets must act in concert to produce a force of arbitrary magnitude and direction on the rotor.

For structural and manufacturability, this sort of magnetic bearing is manufactured with iron connecting the horseshoes, so that the stator iron is one monolithic piece. This geometry is regard as an equivalent to eight - poles MB as shown in Figure (1).

Consider this magnetic circuit with N turns of wire around each leg (pole) of the bearing, then source of strength is NI , nominal air gap g between the

rotor and the tip of each leg of the bearing, *a* is the cross-sectional area of each leg, reluctance R. One can solve for the magnetic flux and forces in this magnetic circuit as [7]:

$$f = \frac{NI}{R} = \frac{\mu_o aNI}{g} \quad \ldots.(1)$$

The magnetic flux density, *B*, in the air gap is the then :

$$B = \frac{\mu_o NI}{g} \quad \ldots.(2)$$

We can now use Maxwell's Stress Tensor to figure out the force. For one pole of horseshoe, the force in terms of flux in the gap is.

$$F = \frac{B^2 a}{\mu_o} \quad \ldots.(3)$$

or

$$F = \frac{\mu aN^2 i^2}{g^2} \quad \ldots(4)$$

In addition, the flux density obtainable in the gap should be limited by the flux that can get down the legs of the bearing. For the core material saturates at a force of Bsat, and then the maximum force that can be produced by a particular bearing geometry is:

$$F_{max} = \frac{B_{sat}^2 a}{\mu_o} \quad \ldots(5)$$

Then the maximum current required in a horseshoe is:

$$i_{max} = \frac{B_{sat} g}{N \mu_o} \quad \ldots.(6)$$

Linear relationships between input and resulting output are important in MB. To show this linearization, consider two opposed horseshoes with currents *i1* and *i2* working together to produce forces along one axis of the bearing. The resultant force when both currents are taken into account and the rotor is centered in the bearing is:

$$F = \frac{F_{max}}{i_{max}^2}(i_1^2 - i_2^2) \quad .. (7)$$

For control purposes, this form should be converted to a linear relationship with a change of variables. The currents *i1* and *i2* can be thought of as being composed of a constant "biasing" component (*ibias*) that doesn't produce any force, in combination with a "perturbation" component (*ipert*) that is proportional to the desired force where:

$$i_1 = i_{bias} + i_{pert} \quad \ldots.(8)$$

$$i_2 = i_{bias} - i_{pert} \quad \ldots(9)$$

To get the maximum load capacity out of the bearing, then

$$i_{bias} = \frac{i_{max}}{2} \quad \ldots(10)$$

With this choice of bias, when the maximum force is being produced by one horseshoe, no force at all is being produced by the opposing horseshoe. Then use these to get the force as:

$$F = F_{max}\left(\frac{i_{pert}}{i_{bias}}\right) \quad \ldots(11)$$

It is possible to linearize the force about the centered position to get the dependence of the horizontal force on position, and then eq. (11) is modified to be:

$$F = F_{max}\left(\frac{i_{pert}}{i_{bias}} + \frac{x}{g}\right) \quad \ldots.(12)$$

Where *x* represents the distance that the rotor is displaced from the centered position, or

$$F = ki\ i_{pert} + kx\ X \quad \ldots.(13)$$

Where*:* ki is current force factor and kx is displacement force factor .

The same analysis can be applied to the other two horseshoes to produce a vertical force.

The power amplifier is regulating the flow of energy by converting low power controller output currents into high power actuator input currents. Thus, trans-conductance operation is generally preferred and the power source would be a current source. These amplifiers are either a linear amplifiers or switching amplifiers

Switching amplifiers are more widely used in MB than linear amplifiers, because of high efficiency and large capacity.

Consider a prototype model of radial AMB system has the parameters evaluated from a similar implemented laboratory model. These parameters are given in table 1 which can be used to develop the system transfer functions.

Using equation (5), the maximum force is then 40 Newton, while the force-current factor (ki) and the force-displacement factor (kx) are equal to 2000 N/Amp and 200 N/mm respectively based on the knowledge of equations (12) and (13).

3. Analysis of MB with PID Controller :

The primary tasks of the controller in MB system are to coordinate the transformation of sensor signals when necessary, and to generate control current requests according to the control algorithm. The controller may also handle output coordinate transformation and biasing of the amplifier signal. These controllers can be either analog or digital. In this work, a digital controller is adopted because it is fastest when performing linear math, can implement nonlinear equations, and easier to implement and modify complex algorithms.

The PID controllers are the most widely used for the feedback control of MB because of simplicity, easy realization, and robustness [8,9].

The controller may exploit the position of the rotor as a popular parameter for feedback control signal. To achieve this, a position sensor for MB applications is required.

There are several types of position sensors that have been used, or have potential to be used, in magnetic bearing applications [10].

The suggested probe sensor in this work is the Hall Effect type. It can be made very small in size at low cost and has high sensitivity to temperature changes compared to other types of sensors. Moreover, the output of the sensor is highly susceptible to magnetic noise.

The transfer function of the final system model is assembled simply by connecting the output of the sensor model to the input of the PID controller model and the output of the controller to the input of the power amplifier and then to the actuator model using standard state space formulation[11] .

The PID controller based simulink window command can be implemented to investigate the MB radial forces in two axes (x,y) and then identifies the stand still and dynamic responses of this system.

The displacement variations is caused by a mechanical unbalance and also by eccentric misalignment of a sensor target with a magnetic bearing rotor. The magnetic bearing is considered as a two simple force constants equation (13) , which is defined with respect to displacement and current.

Figure (2) shows the block diagram of a MB and its controller for one-axis magnetic suspension. The position x of a suspended object is detected and amplified by a displacement sensor with gain ksn and then compared with the position reference x*. The error is amplified by a controller Gc and fd is the disturbance force of this axis.

The transfer function of this system is derived to be [12]:

$$\frac{x}{x^*}=\frac{(K_p+sT_d)k_ik_{sn}}{(K_pk_ik_{sn}-k_x)+T_dk_ik_{sn}s+ms^2} \quad \ldots(14)$$

Solving a characteristic equation for S gives two poles which shows that a derivative controller is necessary to make the magnetic suspension feedback system is stable.

The magnetic suspension system can be modified by adding the disturbance force *fd* , the object displacement x, and speed. The dynamic stiffness is:

$$\frac{x}{f_d}=\frac{1}{ms^2+T_dk_ik_{sn}s+K_pk_ik_{sn}-k_x} \quad ..(15)$$

In practice, kx usually has variations and fluctuations caused by bias current and nonlinearity. Therefore Kp, ki, and ksn should be carefully selected to be significantly higher than kx .

The system responses is well investigated for a given proportional gains *kp*, derivative gains kd. The PID controller with gain G_c is developed by adding an integrator *Kin/s* to a PDC. The best displacement response is achieved with an optimum step disturbance force of Kin = 10 000 [12].

In an actual magnetic suspension system there are many causes of possible delay caused from iron losses, eddy current, saturation, the first order lag element of a winding resistance and inductance, and Limited frequency response of a current driver and sensor.

For two axes magnetic suspension system , the generated radial forces are aligned on two perpendicular axes which usually coincide with the x- and y-axis displacements.

There are several interference caused by the following sources :

-The two axes may not be aligned .

-Electro-magnet of a radial magnetic bearing is constructed with a misalignment at an angle with respect to the radial displacement sensors.

-The direction of the generated radial force has an angular position error.

The interference radial forces can be written as:

fdmy = Kmx fNFBx …(16)

fdmx = Kmy fNFBy …(17)

where fNFBx and fNFBy are the feedback radial forces, and

$$Kmx = -\sin q_{er} \quad \ldots (18)$$

$$Kmy = \sin q_{er} \quad ..(19)$$

q_{er} is the delayed angular position.

Figure 3 shows a block diagram of the controlled MB system includes the interference between the two axes. The interference is generated by Kmx and Kmy which is important to be analyzed.

The output radial positions x,y are compared with the corresponding radial position references and then amplified by PID controller gain Gc and ki .

A disturbance forces fdmx, fdmy is added to the feedback radial forces and the sum is applied to the magnetic bearing system Gp.

It is important to consider the case where the two forces are unbalanced through the rotation of the shaft. The x-y axes are perpendicular axes in a stationary frame. The shaft is perfectly symmetrical but there is an additional mass of (*me*) at a radius of (e) in the direction of $w_{rm}t$, where w_{mr} is the rotational angular speed of the shaft. The radial forces in the two perpendicular axes are defined by :

$$Fx = me e w_{rm}^{2} \cos w_{em} t \quad \ldots (20)$$

$$Fy = me\, e w_{rm}^{2} \sin w_{rm} t \quad \ldots (21)$$

A simplified block diagram considering the unbalanced radial force is shown in figure (4) . It consists of PID controller, sweep generators , sensor gain and the MB .. The sweep generator generates unbalanced disturbance radial forces f_{dx} , f_{dy} added to the negative feedback forces f_{NFBx} and f_{NFBy} .

Open loop transfer function of AMB is obtained using the previous values of ki , kx and the rotor mass *m* then:

$$G(s) = \frac{200}{4s^2 - 2*10^6} \quad \ldots (22)$$

PID controller transfer function Gc(s) can be deduced for an optimum values for PID parameters (Kp =10 , Kin =1000 , Td = 0.01) :

$$Gc = 10 + \frac{1000}{s} + \frac{0.01s+1}{10^{-4}s+1} \quad \ldots (23)$$

The transfer function for influence of delay causes by the first order lag element of a winding resistance and an inductance is :

$$G_d = \frac{1}{10^{-3}s + 1} \quad \ldots (24)$$

The final transfer function of AMB system is : , G(s) . Gc(s) . Gd(s) , with feed back of the gain sensor ksn . To get a suitable ksn, the values of *s* is obtained from the root locus of the MB system as

shown in figure (5) . The root locus shows the system is stable when the value of ksn between (1500 – 6500) and maximum damping factor at(ksn =2500)

4. Analysis of MB with NN controller

There are three popular neural network architectures that have been implemented in the NN Toolbox of MATLAB software :

a- Model Predictive Control

b- NARMA-L2 (or Feedback Linearization) Control

c- Model Reference Control

NARMA-L2 controller is simply a rearrangement of the NN plant model, which is trained offline in batch form, so it is the best technique to be proposed in this work. The only online computation is a forward pass through the NN controller. The NARMA-L2 software is used for training this controller and to decoupling the interferences between the two axes radial forces .

It is referred as feedback linearization when the plant model has a particular form (companion form) and it is referred to as NARMA-L2 control when the plant model can be approximated by the same form. The idea of this type of control is to transform nonlinear system dynamics into linear dynamics by canceling the nonlinearities.

The identification of the system by this controller can be summarized by the flowing steps:

- Identify the system to be controlled. Neural network is trained to represent the forward dynamics of the system. One standard model that has been used to represent general discrete-time nonlinear systems is the Nonlinear Autoregressive-Moving Average (NARMA) model [13]:

$$y(k+d) = N[y(k),y(k-1),\ldots, y(k-n+1), u(k),u(k-1),\ldots,u(k-n+1)] \quad (25)$$

where $u(k)$is the system input, and $y(k)$is the system output.

- Make the output system follows some reference trajectory by developing a nonlinear controller of the form:

$$y(k+d) = yr(k+d) \quad (26)$$

$$u(k) = G[y(k),y(k-1),\ldots, y(k-n+1), yr(k+d),u(k-1),\ldots,u(k-m+1)] \quad (27)$$

To implement the controller model with NARMA-L2, one solution is to use approximate models to represent the system[14]:

$$\hat{y}(k+d)=f[y(k),y(k-1),..,y(k-n+1),u(k-1),..,u(k- . m+1)]+ g[y(k),y(k-1),,y(k-n+1),u(k- . 1),,u(k-m+1)]u(k) \quad (28)$$

Where the next controller input is not contained inside the nonlinearity. The advantage of this form is that controlled input make the system output follows the reference equation (26) .

Figure (6) shows the block diagram of NARMA-L2 controller together with the reference model and the plant,. The controller makes (*ec*) [The difference between plants output (y) and the reference (yr)] very small by evaluated input plant (u) .

Figure (7) shows the complete MB controller system that can be implemented with the previously identified NARMA-L2 plant model.

5. The simulation models

To obtain the simulation results of the MB response, then a three main Simulink models are developed and implemented. Figure (8) shows the 1st model of MB system in one axis using the PID controller only ,where :

Fcn1 represents the open loop transfer function for electromagnetic force of MB as represented in equation (22).

- Gain 1, Fcn3, and Fcn2 represent the PID controller transfer function as (*G*c) in equation (23) , and (Gain 3) represents the controller gain.
- Fcn represents the transfer function for influence delay (*Gd*) of equation (24)
- Gain(-K-) represents the gain sensor (*k*sn)
- chirp Signal (sweep signal) and Gain 4 represent the influence interferences force (*f*d) , it is a sine wave depends on the variable speed of the rotor as illustrated in equation (20).
- Step represents the displacement of x-axis .

- Gain 2 represents the gain for Scope 1 which shows the time response of system in this simulation.

The 2nd model is shown in Figure (9). It is a modified model to improve the MB response in one radial axis by adding the NN - NARMA-L2 Controller to the PID controller. The implementation is achieved by copying the NARMA-L2 Controller block from the NN Toolbox and then how the NARMA-L2 controller is trained to stored the transfer function of MB system with PID controller in Linear Time Invariant term (LTI System) .

Figure (10) shows the 3rd simulation model of the MB system for two radial (X-Y) axes controlled by both PID and NN , where :

- A NARMA L2 for each axis , and (LTI System) for x-axis and (LTI System 1) for Y-axis
- The (Chirp Signal and Gain4) is an interferences displacement distortion for x-axis and (Chirp Signal1 and Gain9) for Y-axis .
- Scope and Scope 2 shows the displacement time response for X and Y respectively .
- Grahp1 X(2Y) shows the rotor location.

6. Simulation Results

In this section, a simulation results for controlling the proposed Radial MB prototype model is presented based on MATLAB (Simulink) algorithm. Firstly by adopting the PID controller and then improving the system response by adding the NNC (NARMA-L2).

Figure (11) shows the y-displacement of the rotor for stand still condition (rotor speed=0) using PID controller only [figure (8)], *fd is* equal zero by remove Chirp Signal. This response shows that the system is stable and the rotor is suspended after 0.025 sec and it approaches the zero position after 0.05 sec.

When the rotor starts to accelerate (from 0 up to 6000 rpm) by programming the Chirp Signal from 0 to 100Hz at only (1sec) . This dynamic state has a coordinate position response using the PID controller only as illustrated in figure (12) for rotor speed of 3000 rpm. A similar response can be obtained in the x-axis.

The position response is improved by adding the NNC to the PIDC. Figure (13) presents the x- displacement response for the stand still condition of the rotor based on the simulation model of figure (9). It shows that the rotor is suspended at zero position after 0.07s while the displacement of the rotor twice of that using only PID controller .In case of the dynamic response of the rotor, then Figure (14 a,b) show the displacement responses in x-axis and y-axes respectively . In this results, the two radial axes are adjusted at a different displacements of x, y axes and the chirp signal has a different values of gains. To show the rotor location in x-y plane , figure (15 a) shows the position of rotor of the system using PID controller only at (stand still response) and figure (15 b) shows the rotor location in x-y plane when adding NN Controller . It is clear that by using NNC, the system is more accurate and fast at zero speed. Figure (16 a) shows the rotor location in x-y plane for a dynamic case using PIDC only and the interferences between the two axes at accelerated speed from (0 to 1500 rpm) ,while figure (16 b) shows the x-y location when adding NNC for a dynamic case where the rotor accelerated (from 0 to 3000 rpm) . It shows that the rotor is adjusted to the centre position as quick as possible when NNC is adopted.

7. Conclusions

This work is concentrated mainly on the controlling performance of the proposed RAMB model. The results obtained tend to the following conclusions:

1- The available force range is one of the most important parameters of the active magnetic bearing and strongly affects the bearing stiffness. The character of the produced electromagnet force has to be taken into linear form during controller

design because of a complex task consisting of analysis of AMB

2- A simulation of linear form model has been developed for closed-loop control of a magnetic bearing plant that along with a PID controller because the system is normally unstable. Also a suitable characteristic using root locus criteria and a quite gain sensor can be obtained.

3- The PID controller uses displacement of the suspended object is necessary to training the NNC (NARMA-L2) because open loop MB system is always unstable and there is a large inherent problem in NNC training without PID controller.

4- Effectiveness of the NN Controller comes from the ability to generate correct position of radial magnetic bearing by decoupling the interferences between the two axes forces and the system don't need any additional controller equipment.

5- Using Neural Network controller with the PID gives an accurate position adjustment. These are cleared by simulation test that leads to minimize withdrew current from power supply, therefore the reliability of the system are increased

6- The software program based on the knowledge of MATLAB algorithm with the application of NARMA L2 as the best NNC type has achieved an accurate feedback controller system.

8. References

[1] E. H. Maslen. Magnetic Bearing Synthesis for Rotating Machinery .PhD thesis, University of Virginia, 1991.

[2] I.A.Griffin , A.J. Chipperfield ,And P.j. Fleming "Active Magnetic Bearing Control System Testing and Validation Using a Multi-objective Genetic Algorithm "pp 1675 -1679 trans. IEEE June 2000

[3] C. E. Lin and H. L. Jou. "Force model identification for magnetic suspension systems via magnetic-field measurement". IEEE Transactions on Instrumentation and Measurement, pp 767-771, April 1993.

[4] H . Habermann and G.Liard " An Active Magnetic Bearing System " ASME Journal of tribology Vol .110 , 1980

[5] Adam plant 'FFEMLAB SOFTWARE APPLIED TO ACTIVE MAGNETIC BEARING ANALYSIS" Int. James Appli Math Comput . science 2004

[6] F. Mazenc M.Dde Queiroz ,M.malisoff, and Gao "Further Results on Active Magnetic Bearing Control With input Suturation" IEEE Transitionon control system technology Vol1 on 5-11-2006

[7] P. E. Allaire, E. H. Maslen, R. R. Humphris, C. R. Knospe, and D. W. Lewis. " Handbook of Lubrication and Tribology Magnetic Bearings" . CRC Press, Virginia 1994.

[8] Brian C. Wilson "Zero- and Low-Bias Control Designs for Active Magnetic Bearings"IEEE Transaction on control system technology, VOL. X, 2003

[9] W.Ruber and B.Lindenau " Magnetic Bearing Control System " Patent US 5565722. 1996

[10] M.dDNoh " Development of a low-cost inductive sensor " proceedings of the Eighth International Symposium on Magnetic Bearing ,August 2002 .

[11]EricMaslen"MagneticBearing" Proceeding of Univ. of VirginiaJune 2000

[12] Akira Chiba, Tadashi Fukao "Magnetic Bearings and Bearingless Drives" proceeding of Newnes is an imprint of Elsevier 2005

[13]Kishan mehpotra ,Chilukuri K-Mohan " Elements of Artificial Neural Networks" proceeding Japan text bock pp.41 ,2001

[14] K.S.Narenda and K. Parthasarathy, "Identification and Control of Dynamical Systems Using Neural Networks," IEEE Transactions on Neural Networks, Val 1 . 1990

Table 1 parameters of the prototype AMB system

Parameters	Values	Unites
Mass *m*	4	Kg
Aria of pole *a*	17	cm^2
Length of gap *g*	1	mm
Inductance of coil	10	mH
Resistance of coil	1	Ohm
Current base *ibase*	10	Amp
Number of turn N/pole	50	Turn

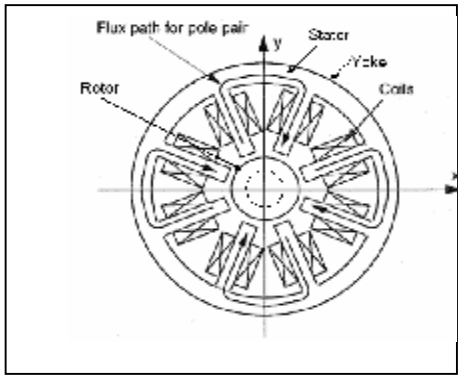

Figure(1)Eight-polesradial magnetic bearing.

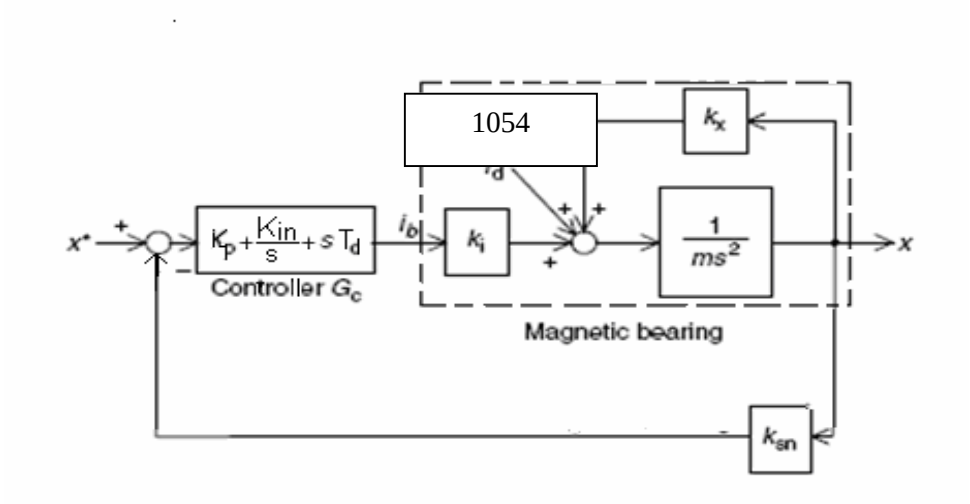

Figure (2) Magnetic suspension system in one axis.

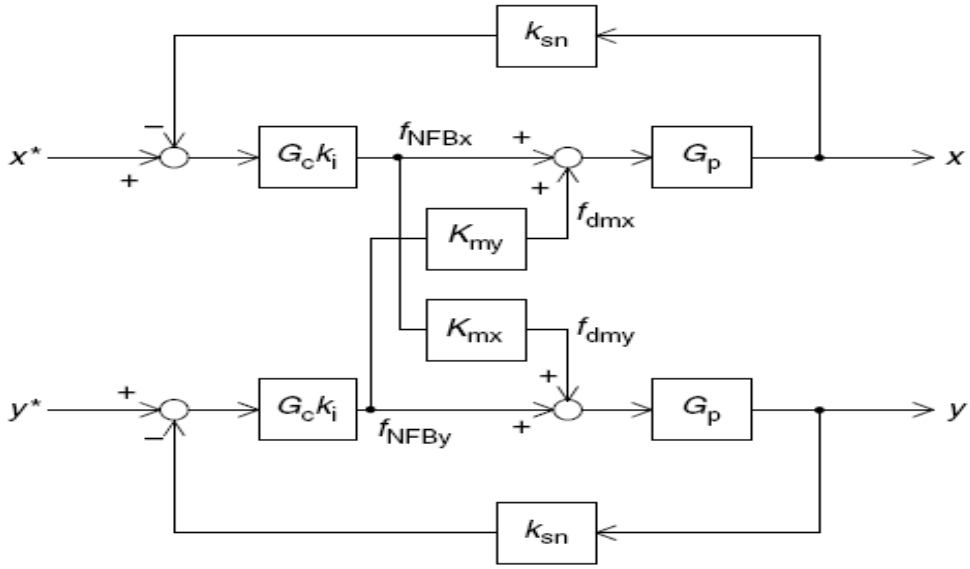

Figure (3) Block diagram of interferences between x - y axes

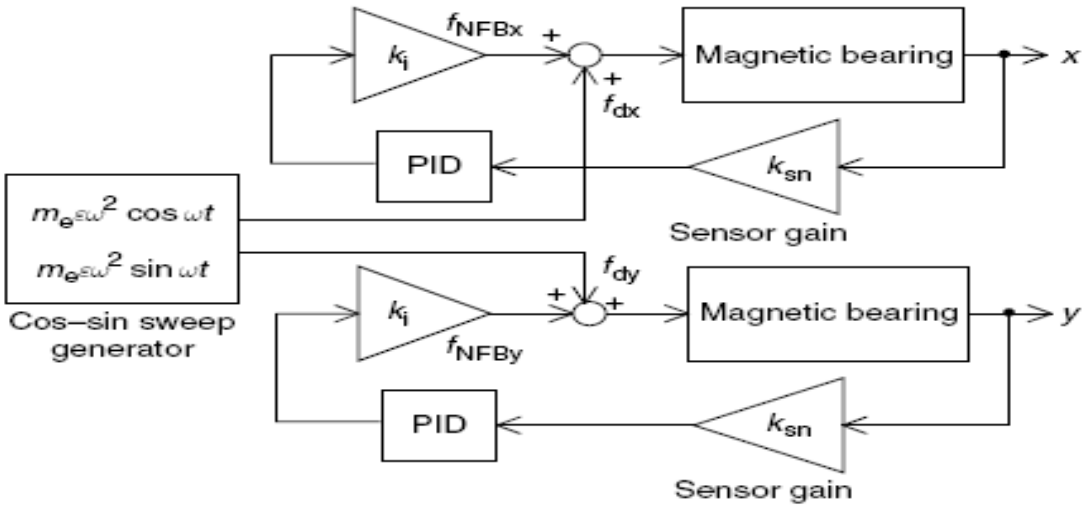

Figure (4) block diagram of unbalance radial forces.

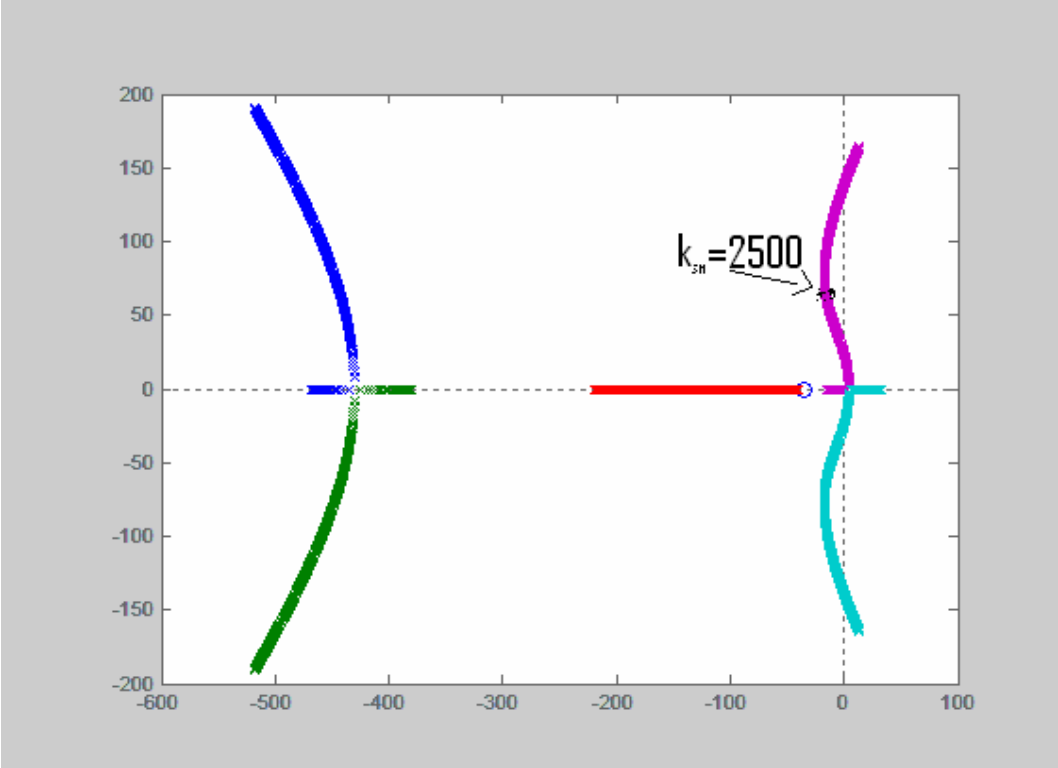

, **Figure (5) the root locus of the MB system**

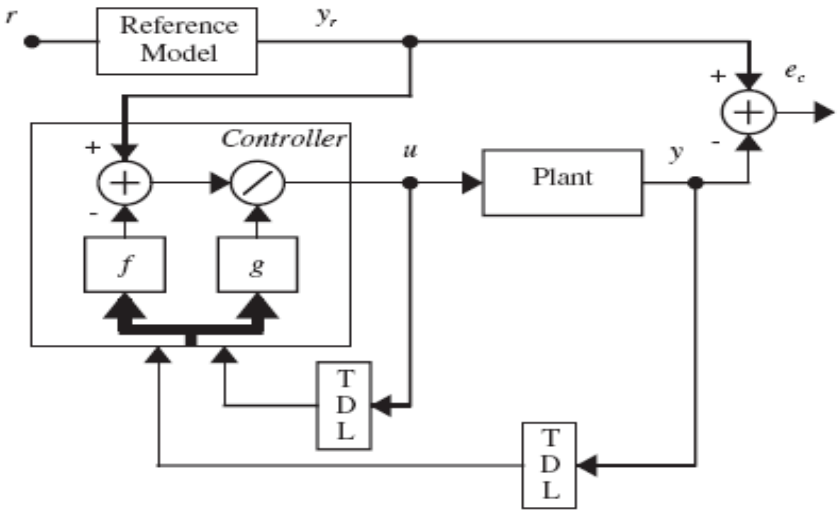

Figure (6) The block diagram of NARMA-L2

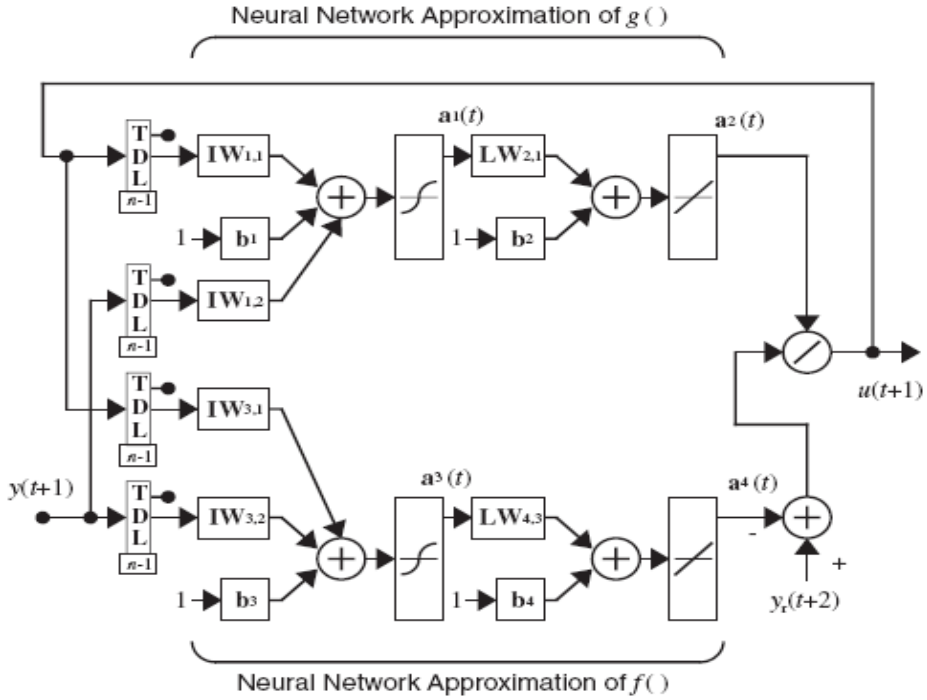

Figure (7) The complete controller system with NN controller NARMA-L2

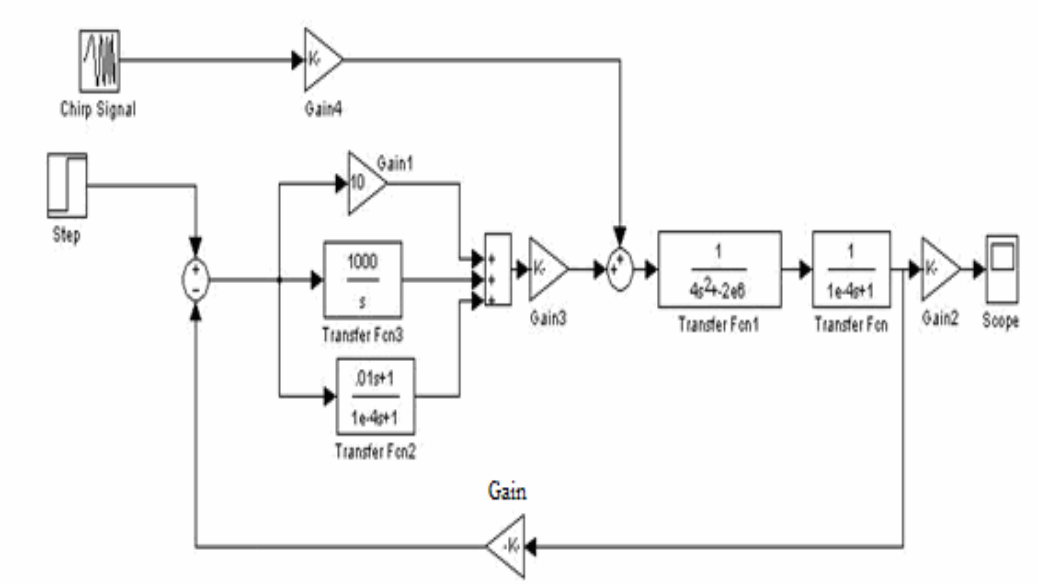

figure 8 Simulation of MB system with PID controller

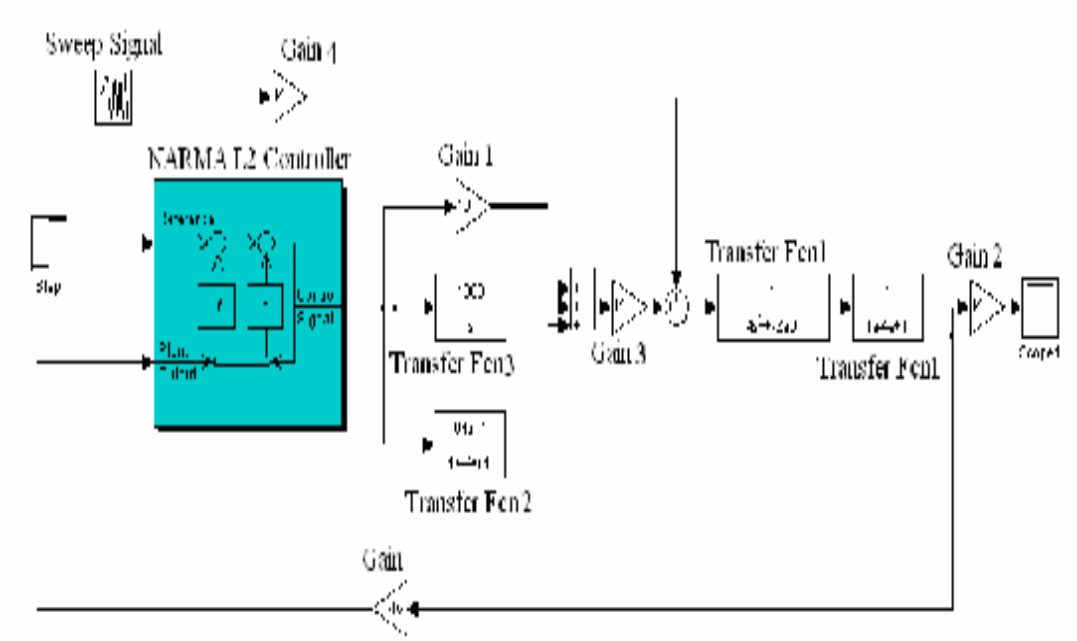

Figure 9 Simulation model MB System With PID Controller And NNC

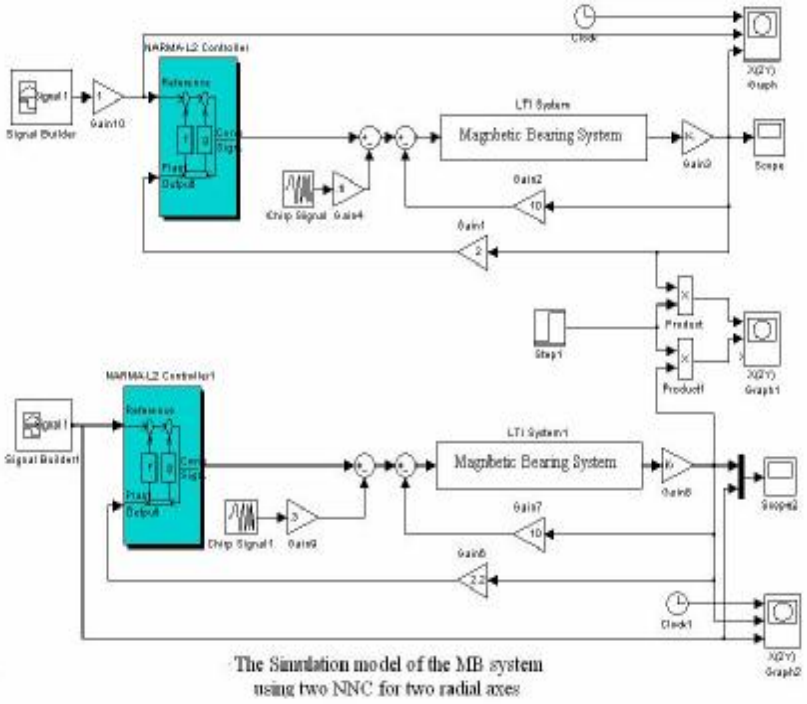

Figure (10) The complete simulation model

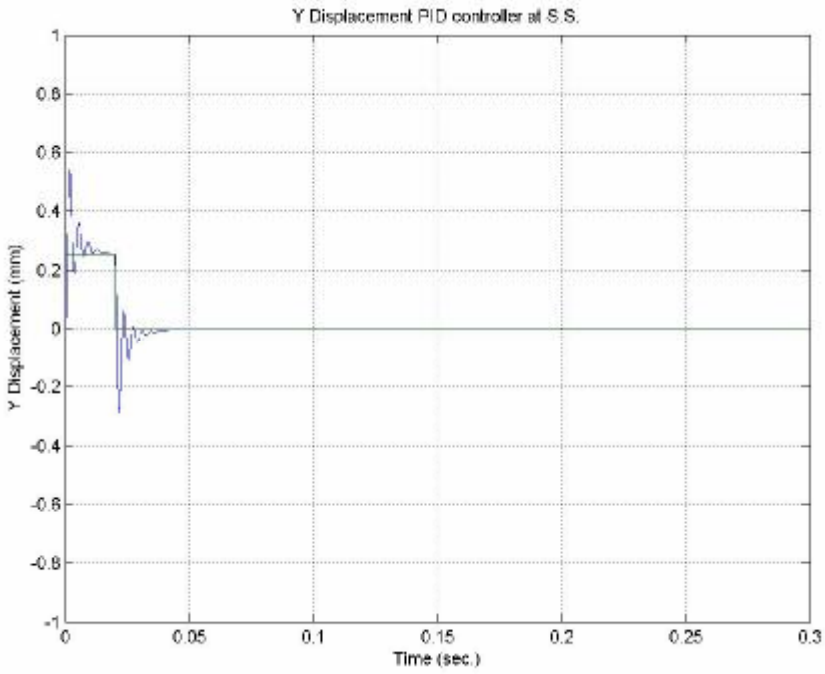

Figure (11) Y displacement stand still response using PID Controller

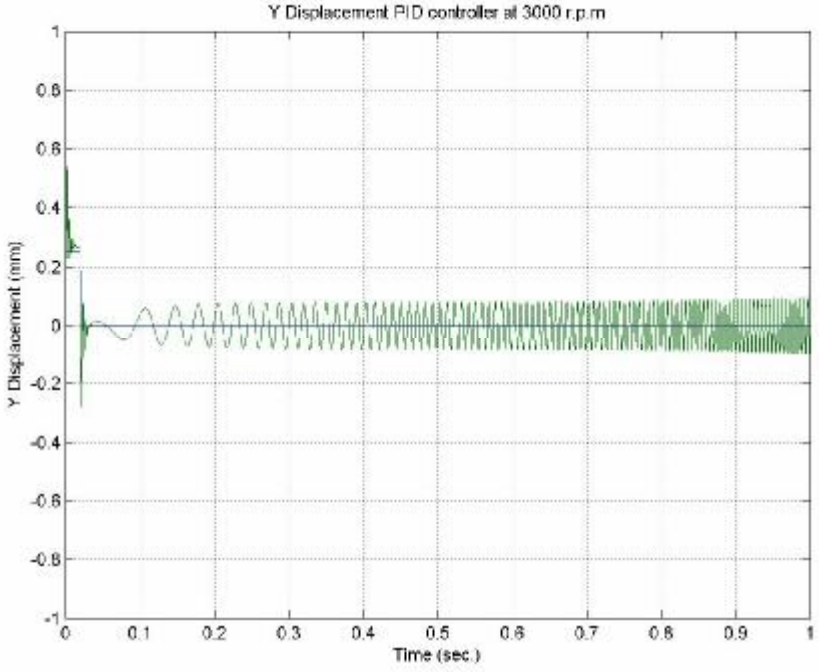

Figure (12) Y displacement time response the rotor accelerated from zero speed to 6000 rpm

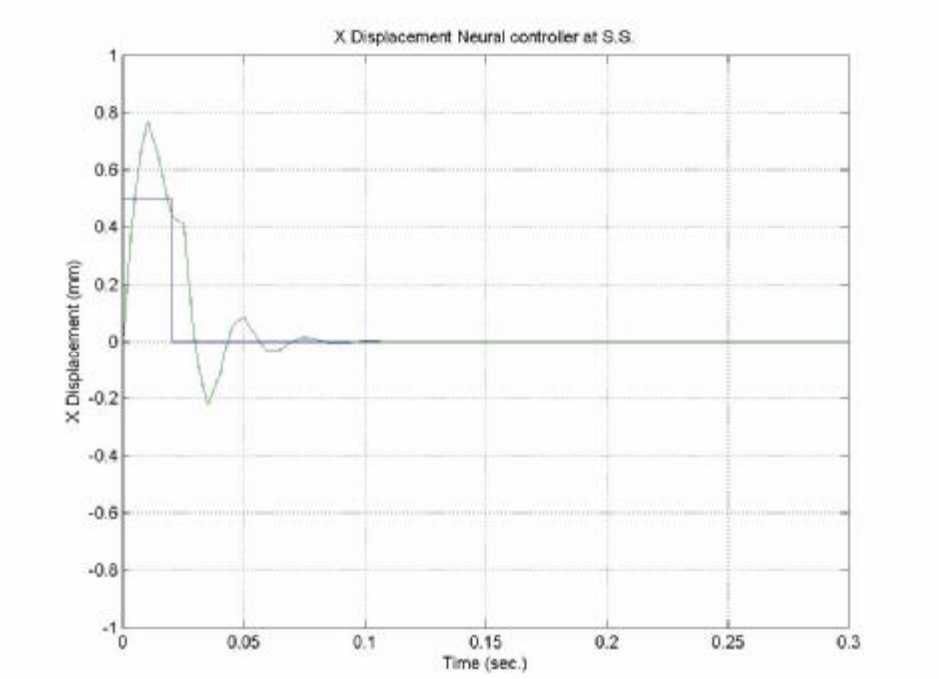

Figure (13) X displacement response static condition using NNC

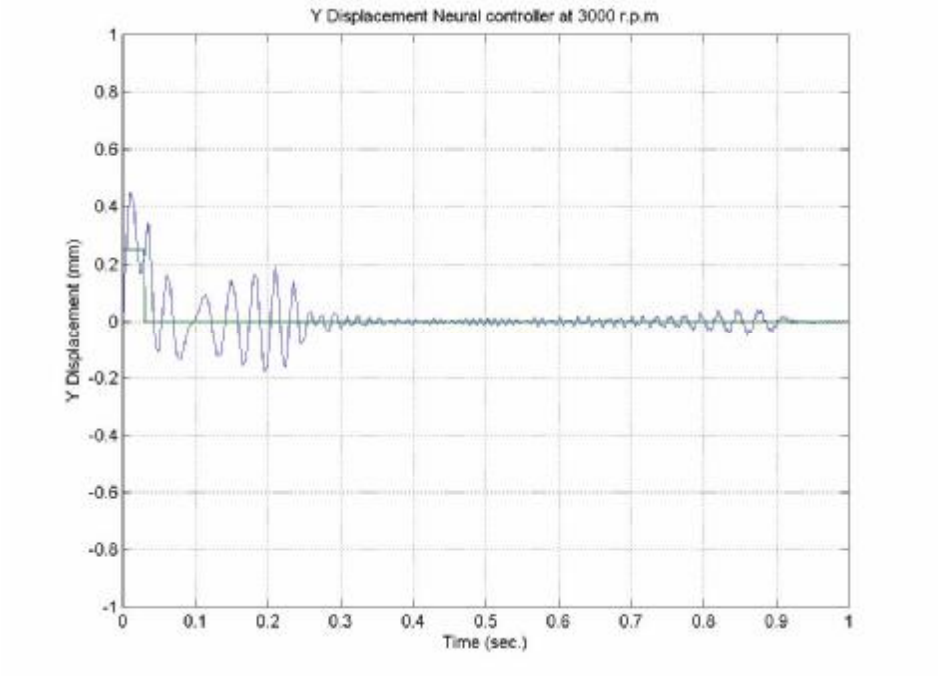

(a)

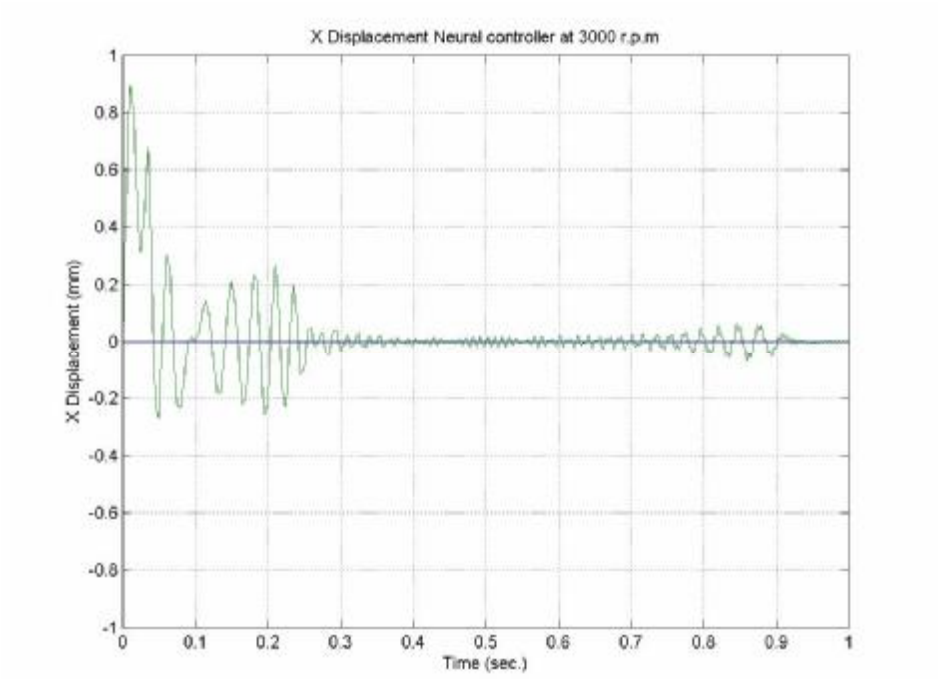

(b)

Figure (14) displacement response for dynamic condition using NNC
a- For Y displacement b- For X displacement

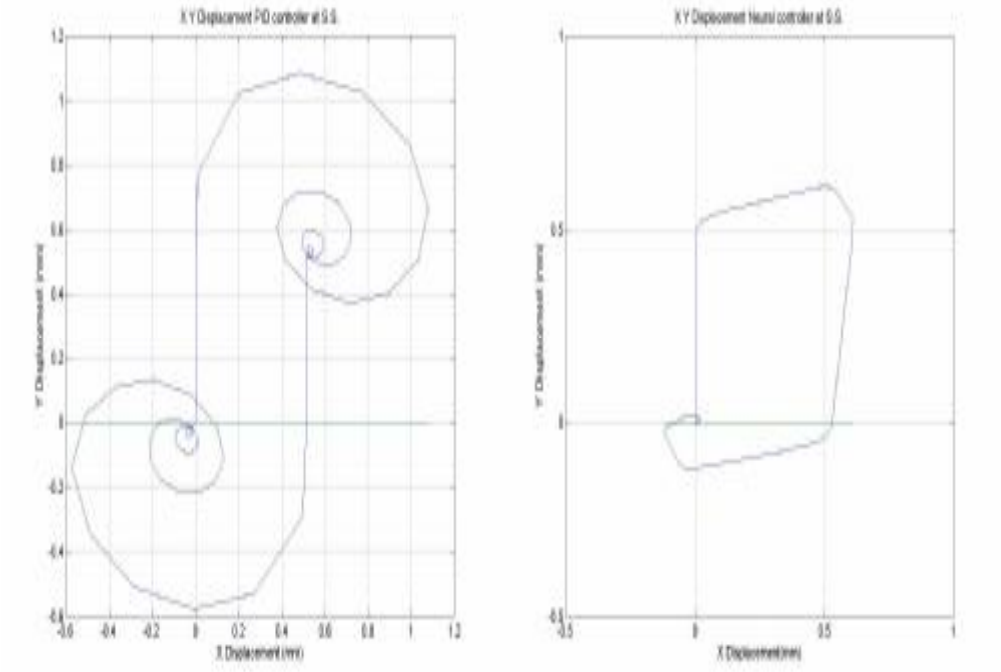

(a) (b)

Figure (15) X-Y rotor locations for static condition .
a- Using PID controller only, b- Using PID with NN controller

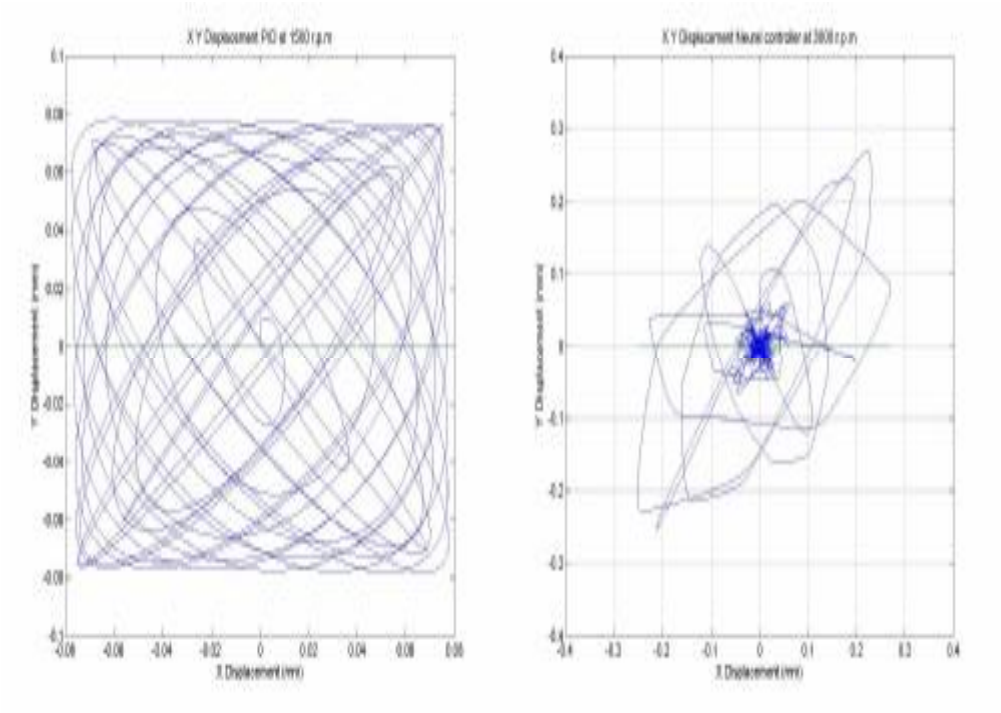

(a) (b)

Figure (16) X-Y rotor locations through the dynamic conditions
a- Using PID controller only . b- With NNC